ACS Catalysis

Research Article

pubs.acs.org/acscatalysis

Selective Deoxygenation of Aldehydes: The Reaction of Acetaldehyde and Glycolaldehyde on Zn/Pt(111) Bimetallic Surfaces

Jesse R. McManus, Eddie Martono, and John M. Vohs*

Department of Chemical & Biomolecular Engineering, University of Pennsylvania, Philadelphia, Pennsylvania 19104-6363, United States

ABSTRACT: Temperature programmed desorption (TPD) and high resolution electron energy loss spectroscopy (HREELS) were used to characterize the adsorption and reaction of acetaldehyde and glycolaldehyde on Zn-modified Pt(111) surfaces. The barriers for both C−H and C−C bond cleavage in adsorbed aldehydes were found to be higher on Pt(111) decorated with Zn adatoms or containing a PtZn near-surface alloy, compared to Zn-free Pt(111). This results in stabilization of aldehydes adsorbed in an η_2(C,O) bonding configuration and hinders formation of acyl intermediates as typically occurs on group 10 metals. Adsorbed η_2(C,O) acetaldehyde and glycolaldehyde on Zn-modified Pt(111) were found to undergo selective C−O bond scission to produce adsorbed hydrocarbon intermediates and hydroxyl groups, while decarbonylation of acyl species to produce CO and hydrocarbon fragments was the primary pathway on the Zn-free surface. These results provide mechanistic insights that are useful for the design of hydrodeoxygenation catalysts for the upgrading of oxygenates derived from biomass, such as glucose and furfural.

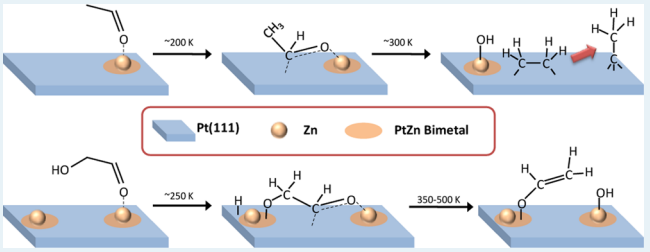

KEYWORDS: *acetaldehyde, glycolaldehyde, ethanol, TPD, HREELS, deoxygenation, hydrogenolysis*

INTRODUCTION

Supported metals play a pivotal role in catalyzing a range of complex hydrocarbon transformations required for the efficient production of fuels and chemicals from petroleum feedstocks. The proposed use of biomass as an alternate, renewable carbon source will also require metal catalysts to facilitate the upgrading of bio-oxygenates, such as glucose and xylose, to useful products.[1−3] While many of the catalytic pathways required for biomass upgrading are similar to those used in petroleum refining, some are unique such as hydrogenolysis of the C−O bonds in aldoses and furfurals, which requires C−O bond scission and selective hydrogenation of C═O and C−OH groups in the presence of aromatic and C═C functionalities. These reactions are particularly important for liquid fuels production from biomass where deoxygenation is necessary.

In most cases, monometallic catalysts are not particularly selective for these bio-oxygenate specific reactions. The use of bimetallics has been proposed as one method to increase and tailor catalyst selectivity,[4−6] and recently, mechanistic studies have started to appear in the literature in which the effect of alloying a highly catalytic metal with a second, less-reactive metal on the selectivity for these reactions has been explored. Examples include Ni-modification of Pt[7−10] and Pd[11] for bio-oxygenate reforming, Co- and Cu- modification of Pt[12] and Ni[13] for hydrodeoxygenation (HDO) of *m*-cresol and furfural, alloying Ru,[14,15] Ag[16] and Pd[17] with Cu for glycerol hydrogenolysis, and Zn modification of Pt[18] and Pd[19−25] for steam reforming of bioalcohols. The differences in reactivity of the bimetallics compared to the monometallics is generally attributed to alterations in the electronic band structure of the metal, and in many cases reactivity trends have been shown to correlate with the energy of the center of the alloy d-band.[7,9,26−29]

While long-range electronic effects in bimetallics are clearly important, it is also possible that the second metal provides specific bonding sites for some intermediates. One such example of this is Sn-modification of Rh for selective hydrogenation of the aldehyde group in propionaldehyde and crotonaldehyde. For this system, Nishiyama et al.[30] have reported that the carbonyl oxygen bonds via donation from the lone pair electrons into locally electron deficient exposed Sn sites. This results in an upright η_1(O) bonding configuration (Figure 1a) for the carbonyl which suppresses interaction of the C═C group with the surface, effectively increasing the selectivity for hydrogenation of the aldehyde group versus the unsaturated C═C bond. Similarly, addition of more oxyphilic atoms like Zn to Pt,[18] Fe to Pt,[31] and Fe to Ni[32] have been proposed to provide specific binding sites for both aldehydes and alkoxides. On the basis of density functional theory (DFT) results for aldehyde adsorption on Fe-modified Ni, Sitthisa et al.[32] have proposed that the Fe atoms provide sites that preferentially bond the carbonyl oxygen in furfural (C_4H_3OCHO), leading to the formation of an η_2(C,O)

Received: May 14, 2013
Revised: June 26, 2013
Published: July 1, 2013

   dx.doi.org/10.1021/cs400355e | ACS Catal. 2013, 3, 1739−1750

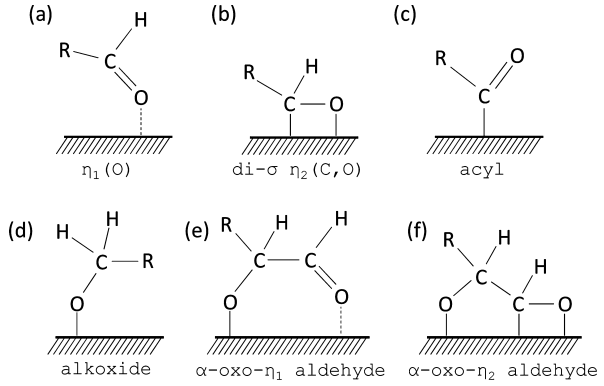

Figure 1. Schematics of surface intermediates: (a) η_1(O) aldehyde, (b) di-σ η_2(C,O) aldehyde, (c) acyl (termed acetyl when R = CH_3), (d) alkoxide, (e) α-oxo-η_1 aldehyde, and (f) α-oxo-η_2 aldehyde.

adsorption complex (Figure 1b) with a weakened C−O bond that facilitates hydrogenolysis to produce 2-methylfuran ($C_4H_3OCH_3$). In contrast, on Ni-only catalysts, less desirable decarbonylation to produce furan predominates. This observation has implications for biomass reforming since HDO of furfurals, which are produced by the dehydration of sugars, is a key step in many of the reaction pathways proposed for the upgrading of cellulosic biomass to value added fuels and chemicals.[33,34]

PtZn bimetallics exhibit some properties similar to those mentioned above for SnRh, and FeNi. In particular, they are highly selective for the hydrogenation of the carbonyl group in α,β-unsaturated aldehydes.[35] We have recently demonstrated that adding Zn to Pt increases the barriers for C−H and C−C scission in adsorbed oxygenates,[18] thereby stabilizing these species to higher temperatures which could help facilitate C−O hydrogenolysis. We have also shown that oxyphilic surface Zn atoms provide bonding sites for adsorbed alkoxides. Whether Zn-modified Pt surfaces are active for hydrogenolysis of carbonyl groups in a manner similar to that observed for FeNi has yet to be explored.

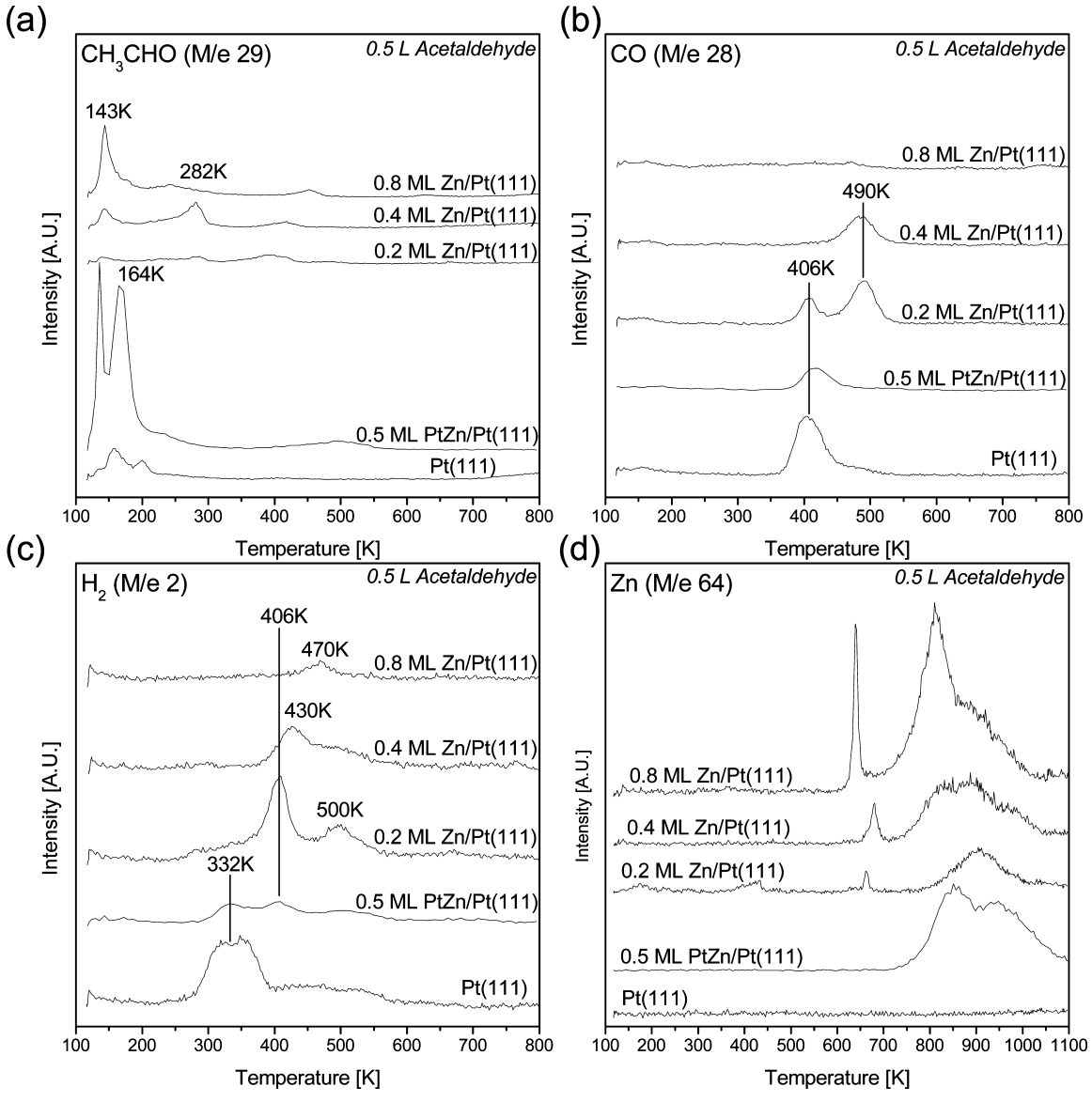

Figure 2. (a) CH_3CHO, (b) CO, (c) H_2, and (d) Zn TPD spectra obtained from Zn-modified Pt(111) surfaces following a 0.5 L CH_3CHO dose. The specific surfaces are indicated in the figure. Note the different temperature scale for panel (d).

dx.doi.org/10.1021/cs400355e | ACS Catal. 2013, 3, 1739−1750

In the work reported herein we have used Zn-modified Pt(111) model catalysts to study the reaction pathways for oxygenates with aldehyde functionalities, namely, acetaldehyde and glycolaldehyde. The latter was chosen as a probe molecule based on previous studies which have shown it to be a good model surrogate for glucose in mechanistic studies of surface reactions.[36,37] Temperature programmed desorption (TPD) and high-resolution electron energy loss spectroscopy (HREELS) data have allowed the stable surface intermediates and pathways to be determined for reaction on both PtZn near-surface alloys on Pt(111) and Pt(111) surfaces decorated with Zn adatoms. Specific sites that are active for C−O bond cleavage in adsorbed aldehydes have been identified and our results provide experimental verification of the HDO mechanism proposed by Sitthisa et al.[32]

EXPERIMENTAL SECTION

Experiments in this investigation were performed using an ultrahigh vacuum (UHV) chamber maintained at 2×10^{-10} Torr, equipped with a quadrupole mass spectrometer (SRS RGA200), an ion sputter gun (PHI electronics), a quartz crystal microbalance (Inficon), and an HREEL spectrometer (LK Technologies). The Pt(111) single crystal substrate (Goodfellow) was 10 mm in diameter and oriented to within ±0.5°. It was cleaned by repeated cycles of 2 kV Ar^+ ion bombardment for 30 min, annealing at 1100 K for 15 min in vacuum, and annealing in 2×10^{-8} Torr O_2 at 1000 K for 20 min. The sample was spot-welded to two tantalum posts connected to the UHV sample manipulator and could be resistively heated and cooled to 100 K by conduction from a liquid N_2 reservoir. HREEL spectra were collected in the specular direction with a 4 eV electron beam directed at 60° with respect to the surface normal, with an elastic peak count rate of between 20,000 and 200,000 cps and a full width half-maximum of 40 cm^{-1}. A heating rate of 4 K s^{-1} was used in all TPD experiments.

Acetaldehyde (Acros Organics, 99.5%) and glycolaldehyde (Pfaltz and Bauer, dimer, 98%) were both introduced from a glass bulb attached to a heated, high-vacuum dosing line connected to the UHV chamber via variable leak valve, as described in a previous publication.[11] The glycolaldehyde source, a crystalline dimer at room temperature, required gentle heating to 330 K to dissociate the dimers and produce sufficient vapor pressure for dosing into the main apparatus. The purity of both the acetaldehyde and the glycolaldehyde reagents was verified using the mass spectrometer on the UHV chamber. Dosages for both molecules used in this study were chosen such that they produced a low-temperature desorption of the weakly adsorbed species, as to ensure surface saturation of the chemisorbed species.

Zn was deposited onto the Pt(111) surface using an evaporative Zn source consisting of a resistively heated tungsten filament wrapped with a coil of Zn wire (Alfa Aesar, 99.99%). The Zn flux was monitored using the quartz crystal microbalance (QCM), and we report the Zn coverages in effective monolayers, where one monolayer is assumed to be the density of Pt atoms on the Pt(111) surface, 1.51×10^{15} atoms/cm^2. All Zn depositions were performed with the Pt(111) sample at or below room temperature. Two types of Zn-modified Pt(111) surfaces were used in this study: (1) surfaces decorated with Zn adatoms prepared by dosing Zn at or below room temperature, which we designate as Zn/Pt(111), and (2) surfaces in which the Zn was incorporated into the near surface region which we designate as PtZn/Pt(111). The latter were prepared by annealing a Zn/Pt(111) surface at 600 K for 2 min. The structure of near-surface PtZn alloys on Pt(111) produced in this manner have previously been characterized in detail by Ho et al.[38] using X-ray photoelectron spectroscopy (XPS), X-ray photoelectron diffraction, and low-energy ion scattering. These studies show that for a PtZn/Pt(111) sample prepared by depositing 1 ML of Zn followed by annealing at 600 K, the surface layer contains only ∼5 at. % Zn, with the balance occupying the second and third layers.

RESULTS

Reaction of Acetaldehyde on Zn-Modified Pt(111) Surfaces. Acetaldehyde TPD experiments were initially performed to probe the reactivity of CHO groups on the Pt(111) and Zn-modified Pt(111) surfaces. Figure 2 shows TPD spectra from acetaldehyde-dosed Pt(111), 0.5 ML PtZn/Pt(111) alloy, and Zn/Pt(111) adatom surfaces with 0.2, 0.4, and 0.8 ML Zn coverages. In each experiment, 0.5 L acetaldehyde was dosed onto the sample at 100 K. For Zn-free Pt(111) (the bottom spectrum in each panel in Figure 2), molecular acetaldehyde desorbed in two peaks centered at 150 and 200 K. Though we monitored for several C_2 products like ethylene, acetylene, ethanol, and ketene, the only gaseous reaction products detected were CO and H_2, which appeared as desorption-limited peaks at 406 and 332 K, respectively. Additional, less-intense H_2 peaks are apparent between 400 and 600 K, which are attributable to the decomposition of surface methyl groups produced during acetaldehyde decomposition at lower temperatures. These results for Pt(111) are consistent with those reported previously in the literature.[39]

The 0.5 ML PtZn/Pt(111) alloy surface was found to be substantially less reactive than Pt(111) with the majority of the acetaldehyde desorbing intact in two sharp peaks centered at 135 and 164 K (Figure 2a). Small amounts of CO and H_2 (Figure 2b,c) were also produced at temperatures similar to that observed for Pt(111). This is consistent with previous studies of the reaction of alcohols on PtZn/Pt(111) alloys where these surfaces were found to be somewhat less reactive than Zn-free Pt(111).[18]

Much more interesting chemistry was observed for the reaction of acetaldehyde on the adatom Zn/Pt(111) surfaces. On these surfaces, desorption of molecular acetaldehyde occurred at 143 K with the size of this peak increasing with Zn coverage. Some small acetaldehyde peaks were also apparent at higher temperatures, the most noticeable being at 282 K for 0.4 ML Zn/Pt(111). The only gaseous reaction products evolved during TPD were again CO and H_2 demonstrating that, like Pt(111), these surfaces are active for both C−H and C−C bond scission. Note, however, that these products tended to be produced at higher temperatures than on Pt(111) suggesting that the Zn adatoms help stabilize the adsorbed intermediates.

For 0.2 ML Zn/Pt(111), CO desorbed in two peaks centered at 406 and 490 K with the latter having roughly twice the area of the former. The peak at 406 K is at the same temperature as that for desorption-limited CO from Zn-free Pt(111). This peak disappeared when the Zn coverage was increased to 0.4 ML or greater, indicating that it corresponds to CO adsorbed on Zn-free portions of the surface. The prominent, higher-temperature CO peak at 490 K decreased in intensity when the Zn coverage was increased to 0.4 ML, and was absent altogether for the 0.8 ML Zn/Pt(111) surface. The fact that

dx.doi.org/10.1021/cs400355e | ACS Catal. 2013, 3, 1739−1750

the intensity of this peak goes through a maximum with increasing Zn coverage suggests that it is associated with species adsorbed on Pt sites that are modified by adjacent or nearby Zn adatoms. Note that since CO was the only carbon-containing gaseous product detected, acetaldehyde decomposition must also result in significant carbon deposition on the surface.

Complex behavior was also observed for the H_2 product during acetaldehyde TPD on the Zn-modified surfaces (Figure 2c). As noted above, the 0.5 ML PtZn/Pt(111) surface had relatively low reactivity toward acetaldehyde, and consequently only small amounts H_2 were produced in a series of overlapping peaks between 300 and 550 K. For the much more active 0.2 ML Zn/Pt(111) adatom surface, H_2 was produced in two large peaks centered at 406 and 500 K with the former being twice the size of the latter. Consistent with the CO desorption spectra, the H_2 peaks became smaller with increasing Zn adatom coverage and also shifted to higher temperatures. Only a single, small H_2 peak at 470 K was present for the 0.8 ML Zn/Pt(111) sample.

Zn desorption spectra were also collected during the acetaldehyde TPD experiments and are shown in Figure 2d. For both the alloy and the adatom surfaces the majority of the Zn desorbs in several overlapping peaks between 700 and 1100 K which is consistent with that reported previously for Zn-modified Pt(111).[18,27,38] Note that the Zn adatoms react with the Pt(111) surfaces to form an alloy between 600 and 700 K during the TPD run, and thus the Zn desorption peaks in the 750−1100 K range are due to desorption of Zn from the alloy surface. For the adatom Zn/Pt(111) surfaces, an additional sharp Zn desorption feature is present between 640 and 680 K. The possible origins of this feature are addressed in the discussion below. These data also provide an additional measure of the Zn coverage for each sample. The relative Zn peak areas for each sample (arbitrarily scaled) are listed in Table 1 and agree well with the amount of deposited Zn as determined by QCM.

Table 1. Relative Zn TPD Peak Areas, Arbitrarily Scaled

surface	Zn peak area
0.8 ML Zn/Pt(111)	0.08
0.4 ML Zn/Pt(111)	0.04
0.2 ML Zn/Pt(111)	0.02
0.5 ML PtZn/Pt(111)	0.05
Pt(111)	0.00

To identify stable reaction intermediates and provide additional insight into the pathways for the reaction of acetaldehyde on the Zn-modified Pt(111) surfaces, HREEL spectra as a function of temperature were collected for surfaces dosed with 0.5 L acetaldehyde and are displayed in Figure 3. For the Zn-free Pt(111) surface at 100 K (Figure 3a), the spectrum is dominated by peaks at 2940, 1700, 1408, 1115, 750, and 523 cm^{-1}, which is consistent with that reported previously by Zhao et al.[39] for acetaldehyde on Pt(111) at 90 K. Mode assignments for each peak in the spectrum are presented in Table 2 and were made via comparison to the infrared and Raman spectra[40] of acetaldehyde and the DFT simulations of acetaldehyde on Pt(111) by Delbecq and Vigné,[41] which are also included in the table. The close correspondence between the HREEL spectra and the DFT simulation demonstrates that the acetaldehyde adsorbs in an η_1(O) configuration in which bonding occurs through the lone pair electrons on the carbonyl oxygen, shown schematically in Figure 1a.

Heating of the sample to 200 K resulted in the disappearance of the ν(C═O) and γ(CH) stretches at 1700 and 750 cm^{-1}, respectively, accompanied by the emergence of a stretch at 1580 cm^{-1} and a shift of the δ(CCO) stretch at 523 cm^{-1} to 607 cm^{-1}, all of which are indicative of C−H scission at the aldehyde carbon and the formation of an acetyl intermediate (Figure 1c). As shown in Table 2, this result is consistent with acetyl formation on Pd(111) reported by Davis et al.[42] Further heating to 300 K and above resulted in decomposition of the acetyl intermediate into CO and H_2, as indicated by the emergence of the peaks at 1816 and 2055 cm^{-1}, which correspond to the ν(C═O) mode of bridge and atop bound CO, respectively, and the appearance of CO and H_2 in the TPD spectra (Figure 2b,c).

For the PtZn/Pt(111) surface alloy, the HREEL spectrum of the acetaldehyde-dosed surface at 100 K, Figure 3b, is nearly identical to that obtained from Pt(111); however, upon heating to 200 K a few notable differences stand out, particularly the emergence of a vibrational loss at 458 cm^{-1} as well as intense losses at 1094 and 1150 cm^{-1}. These peaks most likely correspond to the formation of a di-σ η_2 surface intermediate, as predicted by Delbecq and Vigné,[41] and as shown schematically in Figure 1b. The frequencies for the di-σ η_2 acetaldehyde intermediate are juxtaposed to the experimental vibrational mode assignments for 0.5 L acetaldehyde on 0.5 ML PtZn/Pt(111) in Table 3. In addition to the peaks for di-σ η_2 acetaldehyde, the spectrum also contains small peaks at 600 and 1580 cm^{-1}, which, as discussed above, suggest the formation of some acetyl species. Upon heating to 300 and 400 K, these surface intermediates decompose similarly to that on Pt(111), forming H_2 and CO products. Unlike on Zn-free Pt(111), however, the CO produced from these reactions only occupies the atop sites, as indicated by a vibrational loss at 2002 cm^{-1} and the lack of losses for bridging species between 1800 and 1870 cm^{-1}. This is consistent with previous studies that have shown that CO prefers the atop sites on PtZn alloy surfaces.[18]

A 0.5 ML Zn/Pt(111) surface was chosen as a representative Zn adatom surface for the acetaldehyde HREELS studies. The spectra obtained from this surface are displayed in Figure 3c. As expected, the spectrum at 100 K is nearly identical to that observed for acetaldehyde on the other two surfaces and is characteristic of molecularly adsorbed acetaldehyde (see Table 3). Unlike the other two surfaces, however, the intact acetaldehyde molecule persists to 200 K with no evidence for C−H bond scission or the formation of an acetyl intermediate. This indicates that the Zn adatoms help stabilize the adsorbed molecular acetaldehyde and apparently increase the barrier for C−H bond scission. This is consistent with that reported for methoxide and formaldehyde intermediates on a Zn-modified Pd(111) surface.[22]

Heating to 300 K, however, did cause significant changes in the vibrational spectrum of the adsorbed species, particularly the emergence of a small loss at 647 cm^{-1} and a relatively intense loss at 1022 cm^{-1}, the disappearance of the aldehyde ν(C═O) stretch at 1705 cm^{-1}, and most strikingly, the emergence of a ν(OH) stretch at 3575 cm^{-1}, which is characteristic of an adsorbed hydroxyl group. The simultaneous disappearance of the aldehyde ν(C═O) stretch and appearance of the hydroxyl ν(OH) peak provide direct evidence for cleavage of the C═O bond. Cleavage of only the C═O bond in acetaldehyde would likely result in the formation of a surface

dx.doi.org/10.1021/cs400355e | ACS Catal. 2013, 3, 1739−1750

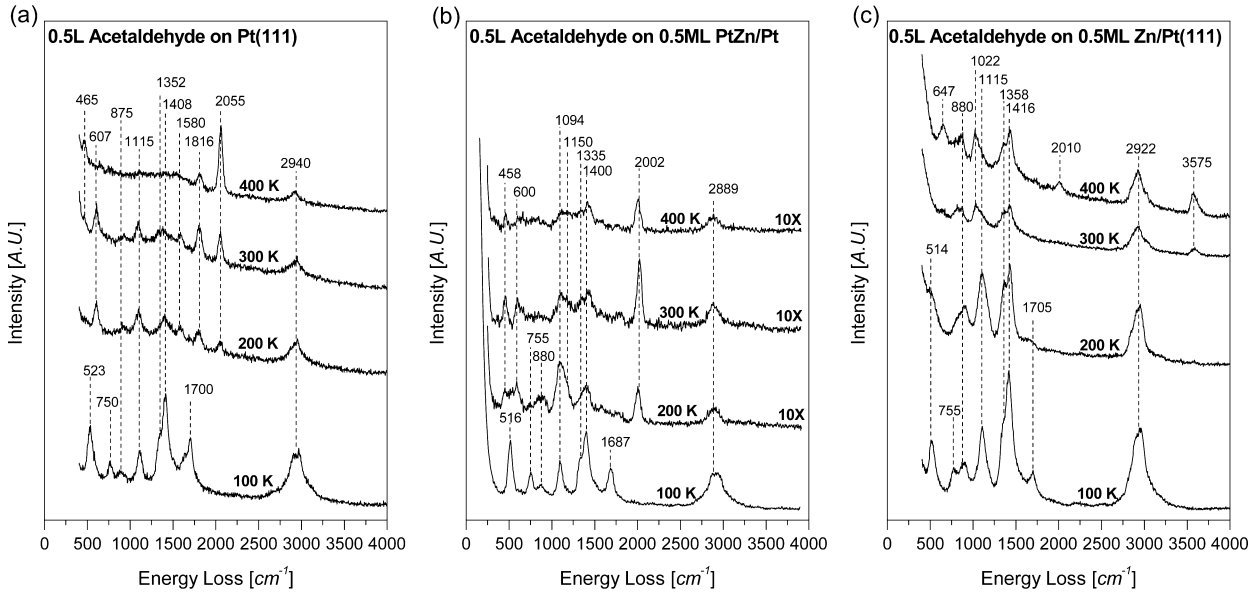

Figure 3. HREEL spectra of 0.5 L acetaldehyde-dosed (a) Pt(111), (b) 0.5 ML PtZn/Pt(111), and (c) 0.5 ML Zn/Pt(111) as a function of temperature.

Table 2. Vibrational Mode Assignments for Acetaldehyde and Acetaldehyde Adsorbed on Various Metal Surfaces[a]

	frequency, cm^{-1}						
	infrared	Raman	Pt(111)	Pt(111)	**Pt(111)**	**Pt(111)**	Pd(111)
mode	vapor[40]	liquid[40]	DFT $\eta_1\mu_1$(O)[41]	90 K[39]	**100 K**	**200 K**	150 K[42]
νCH_3, νCH_2	2967	2964	2968	2984	**2940**	**2940**	2990
$\nu C{=}O$	1743	1714	1682	1667	**1700**		
$\nu_{acetyl} C{=}O$						**1580**	1565
δCH_3	1441	1426	1410	1430	**1408**	**1408**	1390
δCH	1352	1342	1357	1365	**1352**		1390
$\rho_a CH_3$, νCC	1122	1100	1100	1130	**1115**	**1115**	1080
$\rho_s CH_3$, νCC	919	911	884	913	**875**	**875**	900
γCH	763	767	762	788[b]	**750**		
$\delta_{acetyl} CCO$						**607**	600
δCCO, νPtO	509	512	503	550	**523**		

[a]Data from this work marked in bold. [b]Peak not assigned in reference.

ethylidene (=CH−CH_3) intermediate. Ethylidene is unstable on most metal surfaces, but when isolable gives rise to a ν(CC) peak near 975 cm^{-1},[45] which is absent in the HREEL spectrum of the acetaldehyde-dosed surface allowing it to be ruled out. Other possible C_2 intermediates include vinyl (−CH═CH_2), vinylidene (=CH═CH_2), ethylidyne (≡C−CH_3), and ethylene (C_2H_2). The vibrational spectrum of both vinyl[46−49] and vinylidene[50] species on metal surfaces contain characteristic $\gamma(CH_2)$, δ(CH), and ν(C═C) peaks between 900 and 1000 cm^{-1}, 1230 and 1280 cm^{-1}, and 1500 and 1600 cm^{-1}, respectively. The absence of these peaks in the spectra obtained from the acetaldehyde-dosed 0.5 ML Zn/Pt(111) surface heated to 300 and 400 K allow these intermediates to also be ruled out. As shown in Table 4, the peaks in the 400 K spectrum at 2922, 1358, and 1115 cm^{-1} match well with the ν(CH), $\delta(CH_3)$, and ν(CC) peaks expected for an ethylidyne intermediate,[43,51−54] suggesting that this species may be formed. This, however, leaves the peaks at 1416, 1022, and 647 cm^{-1} in the spectrum of the acetaldehyde-dosed sample unaccounted for. These peaks do align reasonably well with those reported previously for ethylene adsorbed in a di-σ configuration with the 1416 cm^{-1} stretch corresponding to a $\delta(CH_2)$ scissor mode, the 1022 cm^{-1} loss to the ν(CC) stretch, and the losses at 647 and 880 cm^{-1} to the $\rho(CH_2)$ and $\tau(CH_2)$ modes, respectively (see Table 4).[43,44,55] Acetylide and acetylene intermediates were also considered[56,57] but provided poor matches with the vibrational spectra of the adsorbed intermediates. These observations lead us to propose that following C−O scission in adsorbed acetaldehyde, both di-σ bonded ethylene and ethylidyne species are formed. In addition to C═O bond cleavage, the production of ethylidyne from adsorbed acetaldehyde also requires cleavage of the carbonyl C−H bond, while formation of di-σ ethylene requires a 1,2 hydride shift. Presumably, the former also provides the hydrogen for the formation of the adsorbed hydroxyl group.

Reaction of Glycolaldehyde on Zn-Modified Pt(111) Surfaces. TPD data obtained from clean and Zn-modified Pt(111) surfaces dosed with 1 L glycolaldehyde are displayed in Figure 4. The primary reaction pathway on Pt(111) is complete dehydrogenation to produce CO and H_2 which appear as desorption-limited peaks at 397 and 320 K, respectively. Small amounts of CH_3OH and CH_2O are also produced at 242 and 320 K, respectively. These products are represented by spectra for m/e 31 and 30 in Figure 4, and were identified based on

dx.doi.org/10.1021/cs400355e | ACS Catal. 2013, 3, 1739−1750

Table 3. Vibrational Mode Assignments for 0.5 L Acetaldehyde-Dosed Zn-Modified Pt(111)[a]

	frequency, cm^{-1}			
	PtZn/ Pt(111)	PtZn/ Pt(111)	Pt(111)	Zn/ Pt(111)
mode	100 K	200 K	DFT di-σ η_2[41]	100 K
νOH				
νCH_3, νCH_2	**2889**	**2889**	2943	**2922**
νC═O	**1687**			**1705**
ν_{acetyl}C═O		**1580**		
δCH_3	**1400**	**1400**	1409	**1416**
δCH	**1335**	**1335**	1359	**1358**
δCH, νCC			1294	
νCO		**1150**	1169	
$\rho_a CH_3$, νCC	**1094**	**1094**	1048	**1115**
$\rho_s CH_3$, νCC	**880**	**880**	914, 827	**880**
γCH	**755**	**755**	914, 827	**755**
δ_{acetyl}CCO		**600**		
δCCO, νPtO	**516**	**516**	546	**514**
νPtC		**458**	427	

[a]Data from this work marked in bold.

Table 4. Vibrational Mode Assignments for Acetaldehyde-Dosed Zn/Pt(111)[a]

	frequency, cm^{-1}		
	acetaldehyde-dosed	ethylidyne[43]	di-σ ethylene[44]
mode	Zn/Pt(111), 400 K	Pt(111)	Pt(110)
νCH	**3034, 2922, 2840**	2950, 2890	2950
δCH_2	**1416**		1430
δCH_3	**1358**	1350	
νCC	**1115**	1130	
νCC	**1022**		1020
ρCH_3, γCH_2		980[b]	960
τCH_2	**880**		805
ρCH_2, ρCH	**647**		670

[a]Data from this work marked in bold. [b]Weak.

analysis of multiple m/e values and their known cracking patterns. Also note that both m/e 30 and 31 are in the mass spectrometer cracking pattern for glycolaldehyde and thus also exhibit a large peak at 183 K which corresponds to molecular glycolaldehyde desorption.

The data for the PtZn/Pt(111) near-surface alloy samples, which were synthesized using 0.1, 0.5, and 1.0 ML of Zn, were similar to that of Pt(111) with the overall dehydrogenation activity decreasing somewhat with increasing Zn concentration. The CO peak did broaden considerably on the alloy surfaces and shifted down to 368 K. This temperature is consistent with that reported for CO-dosed PnZn/Pt(111) indicating that it is desorption limited.[38] The H_2 peak also broadened, and shifted up in temperature to 368 K. As was the case for Pt(111), small amounts of CH_2O (356 K) and CH_3OH (273 K) were also observed for the acetaldehyde-dosed PtZn/Pt(111) surfaces.

Consistent with TPD results for acetaldehyde, significantly different chemistry was observed for the reaction of glycolaldehyde on Zn/Pt(111) Zn-adatom surfaces compared to PtZn/Pt(111) and Pt(111). As shown in Figure 4, which includes data for 0.1 and 0.4 ML Zn/Pt(111) dosed with 1 L glycolaldehyde, the low-temperature peaks corresponding to molecular glycolaldehyde are dramatically reduced in intensity relative to PtZn/Pt(111) and Pt(111), while at the same time the primary reaction products, CO and H_2, are produced at significantly higher temperatures compared with these other surfaces. For the 0.1 ML Zn/Pt(111) both CO and H_2 are produced in two peaks centered at 418 and 535 K. This result is analogous to that observed for acetaldehyde (and also that reported for surfaces dosed with formaldehyde and methanol[18]), though the high-temperature peak for glycolaldehyde is approximately 40 K higher, indicating a slightly increased barrier for decomposition of glycolaldehyde to CO and H_2 compared to acetaldehyde. Again, similar to the acetaldehyde results, the 0.4 ML Zn/Pt(111) sample only exhibited the higher-temperature, reaction-limited CO and H_2 peaks at 531 K. This result further indicates that the Zn adatoms help stabilize the surface intermediates to higher temperatures. Unlike the PtZn alloy sample, the Zn/Pt(111) adatom samples do not produce appreciable amounts of formaldehyde or methanol from glycolaldehyde as shown in Figure 4d and e, again supporting the conclusion that the Zn adatoms stabilize the surface intermediates and prevent low-temperature C−C scission.

For the glycolaldehyde-dosed Zn adatom surfaces, a relatively small quantity of a side product which gave rise to peaks at 215 K in the m/e 45 and 43 spectra with a 1.25 intensity ratio was observed (see Figure 4f and Table 5). Peaks at other m/e values were not observed above the baseline level of the spectra. The most likely species that would give rise to significant m/e 45 and 43 signals are isopropyl alcohol and acetoin ($C_4H_8O_2$), although it seems unlikely that either of these would be produced via the surface reaction of glycolaldehyde. We, therefore, postulate that one of these molecules may be present as an impurity in the glycolaldehyde sample.

HREEL vibrational spectra as a function of temperature for clean Pt(111), 0.5 ML PtZn/Pt(111), and 0.4 ML Zn/Pt(111) dosed with 1 L glycolaldehyde are displayed in Figure 5a,b,c, respectively. The spectra for glycolaldehyde on Pt(111) are similar to those reported previously[37] and show the presence of molecular glycolaldehyde at 115 K. Individual peak assignments are given in Table 6. For comparison, the reported vibrational peak positions and assignments for glycolaldehyde vapor[58] and glycolaldehyde physisorbed on Pd(111)[36] are also included in the table. Heating the glycolaldehyde-dosed Pt(111) surface to 200 K caused two notable changes in the HREEL spectrum, the disappearance of the ν(OH) peak at 3377 cm^{-1} and a shift in the position of the ν(C═O) peak from 1715 to 1610 cm^{-1}. The former demonstrates the dissociation of the O−H group, while the latter is indicative of the carbonyl group bonding to the surface in the η_1 configuration shown in Figure 1a. Heating to 300 K results in C−C bond scission, as evidenced by the decrease of the ν(CC) peak at 917 cm^{-1} and additional dehydrogenation as evidenced by the emergence of peaks at 2039 and 1791 cm^{-1} which are indicative of the ν(CO) mode of atop and bridging CO species. Further decomposition is apparent at higher temperatures and the spectrum at 400 K contains losses indicative of adsorbed CO and small hydrocarbon fragments.

The spectrum of the glycolaldehyde-dosed PtZn/Pt(111) alloy surface at 115 K was similar to that obtained for Pt(111) and contains peaks consistent with physisorbed glycolaldehyde (see Table 6). Heating to 200 K results in the decrease in intensity of the ν(OH) peak at 3386 cm^{-1}, the emergence of a weak ν(C═O) stretch at ~1640 cm^{-1}, characteristic of an η_1 aldehyde, as well as the disappearance of the loss at 620 cm^{-1}.

dx.doi.org/10.1021/cs400355e | ACS Catal. 2013, 3, 1739−1750

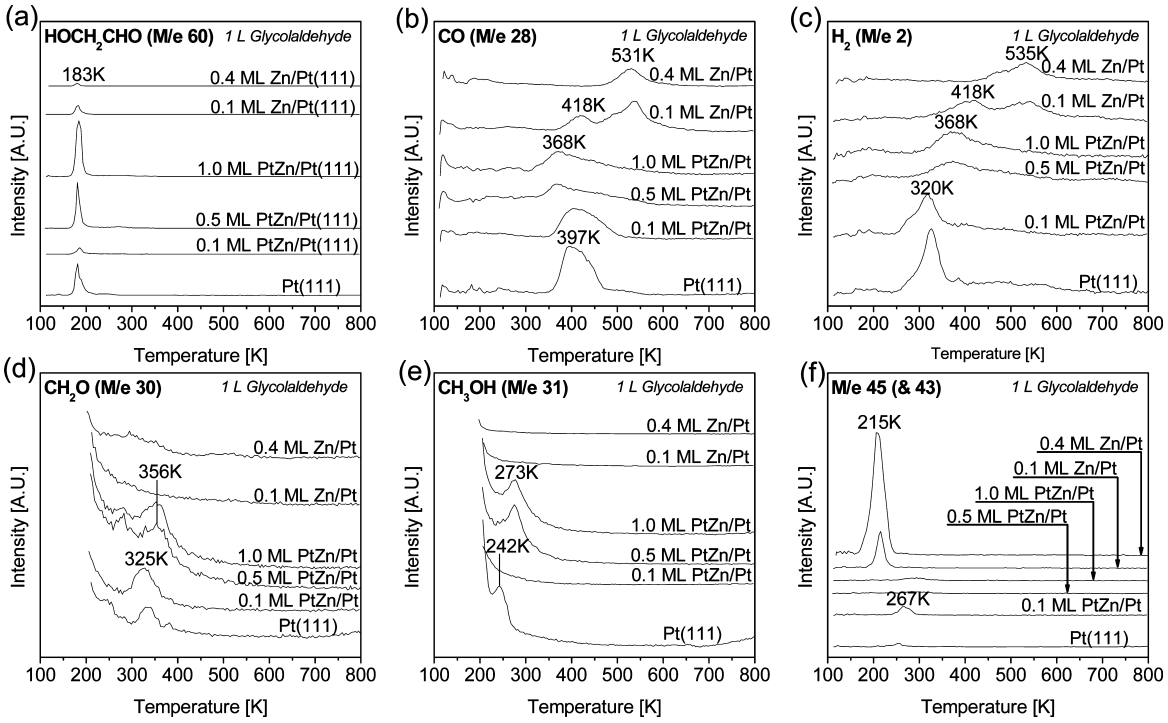

Figure 4. TPD spectra obtained following a 1 L glycolaldehyde dose on various Zn-modified surfaces. Desorption products include (a) $HOCH_2CHO$, (b) CO, (c) H_2, (d) CH_2O, (e) CH_3OH, and (e) an undetermined product with m/e fragments 45 and 43.

Table 5. TPD Product Yields from 1 L Glycolaldehyde-Dosed Zn-Modified Pt(111) Surfaces[a]

	CO	MeOH	CH2O	m/e 45	glycolaldehyde
0.4 ML Zn/Pt(111)	0.25		0.04	0.07	0.02
0.1 ML Zn/Pt(111)	0.59			0.01	0.10
1.0 ML PtZn/Pt(111)	0.51	0.26	0.09		0.68
0.5 ML PtZn/Pt(111)	0.49	0.26	0.06		0.34
0.1 ML PtZn/Pt(111)	0.55		0.10	0.00	0.10
Pt(111)	0.61	0.16	0.03		0.39

[a]Data is arbitrarily scaled.

These changes are also similar to those observed for Pt(111) and indicate that the glycolaldehyde molecule can undergo O–H scission to form an alkoxide intermediate, shown schematically in Figure 1d, or bond to the surface via the lone pair electrons of the carbonyl oxygen. If both interactions occur simultaneously, an α-oxo-η_1(C═O) intermediate would be formed (Figure 1e). This would constrain the molecular backbone somewhat, which might account for the disappearance of the δ(CCO) loss at 620 cm^{-1}. Also note that the continued presence of the γ(CH) stretch at 745 cm^{-1} argues against acyl formation.

Further heating to 250 and 300 K sees the disappearance of the ν(C═O) and ν(OH) stretches and the emergence of the stretch at 2017 cm^{-1} characteristic of atop CO. Additionally, between 250 and 300 K, the intensity of the ν(CC) peak at 853 cm^{-1} considerably decreases which is consistent with C–C bond scission and CO formation. This result is also consistent with the TPD data which show the production of small amounts of formaldehyde and methanol in this temperature range. Continued heating to 350 K and above results in the shift of the peak at 507 cm^{-1} to 446 cm^{-1}, the decrease in intensity of all the glycolaldehyde-related peaks, the persistence of the atop-site CO loss at 2017 cm^{-1}, and the beginnings of a small peak at 1758 cm^{-1} associated with some bridge-site CO, all consistent with the decomposition of the surface intermediates to CO and H_2.

Figure 5c displays the HREEL spectrum for the 1L glycolaldehyde-dosed 0.4 ML Zn/Pt(111) adatom surface, which displays chemistry that differs from that of the clean Pt(111) and PtZn alloy surfaces. At 115 K, the vibrational losses are again characteristic of adsorbed glycolaldehyde with vibrational mode assignments listed in Table 6. Intact OH groups are shown by the peak at 3353 cm^{-1}, and an intact aldehyde group is demonstrated by the ν(C═O) at 1705 cm^{-1}. As shown by the TPD data, heating to 200 K causes desorption of weakly adsorbed molecular glycolaldehyde, resulting in a vibrational spectrum indicative of the chemisorbed species. The main new features in this spectrum include a decrease of the ν(OH) stretch at 3353 cm^{-1}, the appearance of a peak at 1656 cm^{-1} indicative of the ν(C═O) mode of an η_1 aldehyde, and strong $\delta(CH_2)$, δ(CH), and ν(CO) losses at 1412, 1341, and 1085 cm^{-1}, respectively. By 250 K, a relatively stable surface intermediate is formed that persists up to 400 K. This intermediate is marked by a lack of peaks in the ν(OH) and ν(C═O) ranges and well-defined peaks at 2855, 1412, 1341, 1216, 1050, 871, and 375 cm^{-1}, with respective assignments in Table 6. The disappearance of the ν(OH) stretch indicates dissociation of the O–H group and the formation of a surface-O bond. The peak at 1050 cm^{-1} can be assigned to the ν(CO) mode of this end of the molecule. This observation is consistent with that reported for methanol on the adatom surface which also dissociates in this temperature range to form methoxide species.[18] Since it seems unlikely that C═O bond cleavage would occur at 250 K, we attribute the disappearance of the ν(C═O) peak at 1656 cm^{-1} to bonding of the carbonyl group with the surface in a di-σ, η_2 configuration. This would be expected to also give rise to a ν(CO) peak near 1085 cm^{-1}. The

dx.doi.org/10.1021/cs400355e | ACS Catal. 2013, 3, 1739–1750

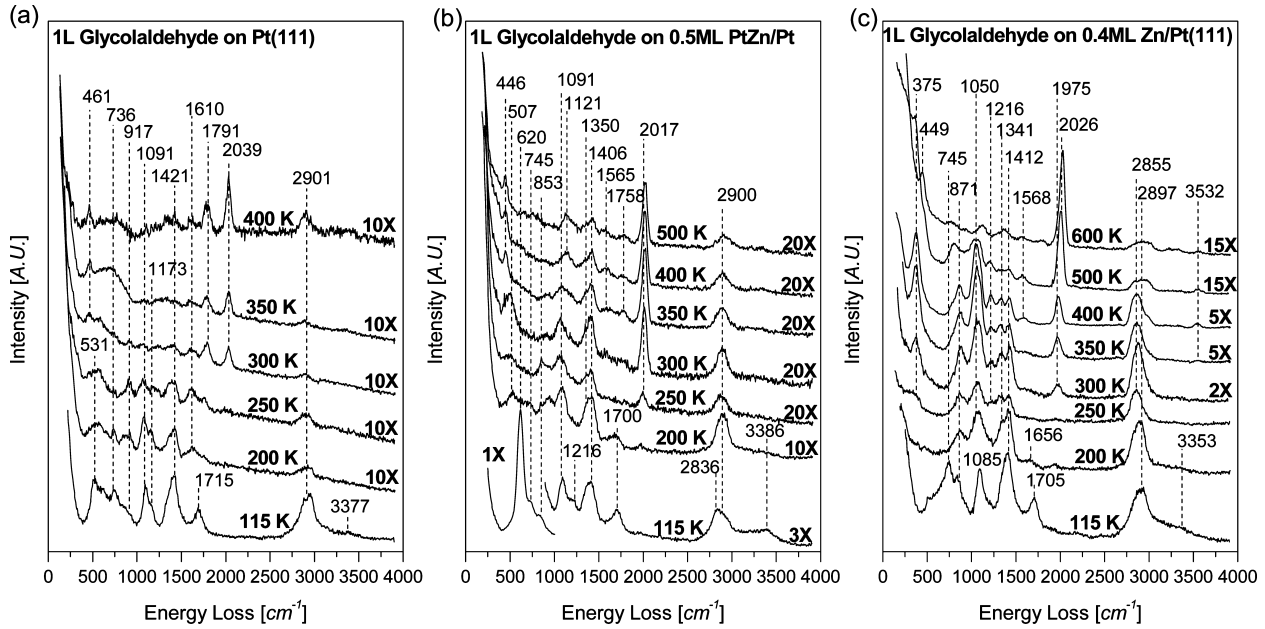

Figure 5. HREEL spectra of 1 L glycolaldehyde-dosed (a) Pt(111), (b) 0.5 ML PtZn/Pt(111), and (c) 0.4 ML Zn/Pt(111) as a function of temperature.

Table 6. Vibrational Mode Assignments for Glycolaldehyde on Various Surfaces[a]

	frequency, cm^{-1}						
	IR[58]	Pd(111)[36]	**Pt(111)**	**Pt(111)**	**PtZn/Pt(111)**	**Zn/Pt(111)**	**Zn/Pt(111)**
mode	vapor	115 K	**115 K**	**200 K**	**115 K**	**115 K**	**250–400 K**
νOH	3549	3315	**3377**		**3386**	**3353**	**3532**
νCH, νCH_2	2881	2827	**2901**	**2901**	**2836, 2900**	**2897**	**2855**
νC═O	1754	1715	**1715**		**1700**	**1705**	
η_1 νC═O				**1610**			
δCH, δCH_2	1425	1390	**1421**	**1421**	**1406, 1350**	**1412**	**1412, 1341**
ρCH_2			**1173**	**1173**	**1216**		**1216**
νCO	1112	1057	**1091**	**1091**	**1091**	**1085**	**1085, 1050**
νCC	859	880	**917**	**917**	**853**	**865**	**871**
γCH, τOH		775	**736**	**736**	**745**	**745**	
δCCO, τOH		639	**620**		**620**	**745**	
νM-O, νM-C			**531**	**531**	**n.r.**	**515**	**375**

[a]Data from this work marked in bold.

intensity of this peak, however, would be relatively small because of the C−O bond axis being oriented nearly parallel to the surface. Together with the alkoxide bonding, this di-σ η_2 aldehyde could assume an α-oxo-η_2 aldehyde configuration, as shown in Figure 1f.

As noted above, the intermediate giving rise to these peaks is relatively stable between 250 and 400 K. A small ν(C═O) peak at 1975 cm^{-1} indicative of atop CO does emerge with increasing temperature, but this peak may be at least partially due to adsorption of CO from the background. There are a few other subtle features in the spectra, especially at 400 K, that suggest the formation of some secondary species. These include the re-emergence of a small peak at 3532 cm^{-1} indicative of the ν(OH) mode of a surface hydroxyl, a shoulder at 3000 cm^{-1} on the ν(CH) peak, and a small peak at 1568 cm^{-1}, which is attributable to either the ν(C═O) mode of an acyl, or perhaps more likely the formation of a C═C double bond. The formation of the surface hydroxyl group suggests C−O scission in a manner analogous to that described above for acetaldehyde on the Zn/Pt(111) surface.

Further heating to 500 K caused additional changes in the $\nu(CH_x)$ peak structure in the 2800−3000 cm^{-1} range favoring the 3000 cm^{-1} peak, as well as a decrease in the intensity of the 1341 and 1050 cm^{-1} peaks and a shift in the 871 cm^{-1} peak to a lower frequency. This, in combination with the relative increase in atop-site CO with respect to the other energy loss peaks, suggests C−C scission and decomposition to CO and H_2. By 600 K, nearly all of the features of the glycolaldehyde intermediates are gone, leaving behind CO and small hydrocarbon fragments.

HREELS of EtOH/0.4 ML Zn/Pt(111). As noted above, there is evidence for C−O bond scission in both acetaldehyde and glycolaldehyde adsorbed on the Zn/Pt(111) adatom surface. For glycolaldehyde, this bond cleavage could potentially occur in either the carbonyl or the alcohol functional groups. To help determine whether this reaction pathway is specific to the carbonyl group, HREEL spectra as a function of temperature were collected for a 0.4 ML Zn/Pt(111) surface dosed with ethanol. These spectra are displayed in Figure 6 and the peak positions and assignments

dx.doi.org/10.1021/cs400355e | ACS Catal. 2013, 3, 1739−1750

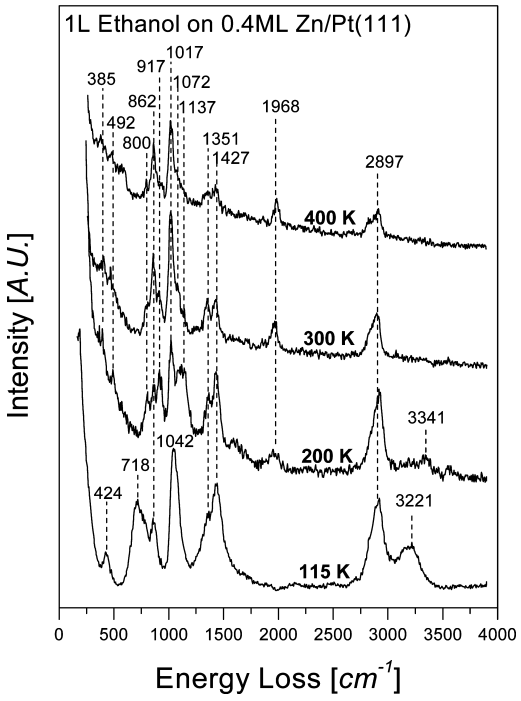

Figure 6. HREEL vibrational spectra for 1 L ethanol on the 0.4 ML Zn/Pt(111) surface.

are listed in Table 7. As emphasized in the table, between 200 and 400 K the spectra are consistent with an adsorbed ethoxide

Table 7. Vibrational Mode Assignments for Ethanol and Ethoxide Species[a]

	frequency cm^{-1}			
	ethanol[8]	**ethanol**	**ethoxide**	ethoxide[56]
mode	Pt(111) 120 K	**0.4 ML Zn/ Pt(111) 115 K**	**0.4 ML Zn/ Pt(111) 400 K**	Pd(111) 200 K
νOH	3230	**3221**		
νCH_x	2960	**2897**	**2897**	2925
δCH_2	1450	**1427**	**1427**	1465
δCH_3	1390	**1351**	**1351**	1400
νCO	1060	**1042**	**1017**	1040
νCC	880	**862**	**862**	855
τOH		**718**		
δCCO	450	**424**	**492**	450
νM-O			**385**	

[a]Data from this work marked in bold.

intermediate[56] and contain the characteristic ν(CO) mode of this species at 1017 cm^{-1}. Upon heating to higher temperatures the ethoxide decomposes to produce CO, H_2, and adsorbed carbon. No C−O bond scission and formation of surface hydroxyls is observed, suggesting the deoxygenation pathway for acetaldehyde and glycolaldehyde is specific to the aldehyde carbonyl.

DISCUSSION

The results of this study provide insight into how Zn atoms incorporated into or adsorbed onto a Pt surface influence the energetics of bond scission and the reaction pathways for adsorbed oxygenates. Consistent with previous studies,[39] acetaldehyde adsorbed on Pt(111) was found to undergo C−H bond scission at the carbonyl carbon to form an acetyl intermediate near 200 K. This species undergoes additional dehydrogenation and C−C bond scission between 200 and 300 K to form CO, H_2, and adsorbed hydrocarbon fragments. In contrast, for PtZn/Pt(111) alloy surfaces, acetaldehyde remains largely intact desorbing at 164 K, with C−H bond cleavage to form an acetyl intermediate being only a minor reaction pathway. The lack of significant acetaldehyde dissociation indicates that either the activation barrier for C−H bond cleavage is higher or the reaction products are less stable on the alloy surface compared to that on Pt(111). For glycolaldehyde the increased production of methanol and formaldehyde between 230 and 350 K, which retain all the C−H bonds in the reactant, also suggests a higher barrier for C−H bond cleavage on the alloy surface. These results are also consistent with that reported previously for the reaction of alcohols on both PtZn/Pt(111)[38] and PdZn/Pd(111)[21,22,24] alloy surfaces.

It is noteworthy that the significant decrease in C−H bond activation on PtZn/Pt(111) compared to Pt(111) occurs in spite of the fact that the outermost layer of the alloy contains only 5% Zn with the remaining Zn being distributed in the second and third layers (see discussion above).[38] This indicates that the change in reactivity of the surface upon Zn incorporation is not due to Zn simply blocking Pt sites, but rather to alteration of the electronic properties of the surface. The fact that large differences were observed for small Zn concentrations also suggests that the Zn induces a relatively long-range electronic effect. This conclusion is similar to that reported previously for Zn-modified Pd(111) surfaces.[21−24,59]

While the alteration of the activity of Pt(111), with respect to acetaldehyde and glycolaldehyde, upon alloying with a small amount of Zn was significant, even more dramatic changes were observed for Pt(111) surfaces decorated with Zn adatoms. Before discussing the reaction pathways observed on these surfaces it is important to recognize that the observed chemistry cannot be attributed solely to adsorption and reaction directly on Zn adatom sites. As we have shown in a previous study of the reactivity of Zn-modified Pt(111) surfaces,[18] monolayer Zn films on Pt(111) are unreactive toward both methanol and formaldehyde with these species adsorbing molecularly at temperatures below 200 K and desorbing intact upon heating. Carbon monoxide was also found not to adsorb on ML Zn films at temperatures above 200 K. The low reactivity of the 0.8 ML Zn/Pt(111) surface toward acetaldehyde observed in the present study is consistent with these previous observations.

In contrast to Pt(111) where acetaldehyde undergoes C−H bond scission at temperatures below 200 K to form an acetyl intermediate which then decomposes to CO, H_2, and adsorbed CH_x between 200 and 350 K, the HREELS results indicate that on Zn/Pt(111) an η_2(C,O) intermediate is formed which remains intact to ∼350 K. Note that this is consistent with the barrier for C−H bond scission being higher on Zn-modified Pt(111) compared to clean Pt(111) as discussed above for the alloy surface. This difference is also readily apparent in the TPD data where the desorption-limited H_2 peak at 332 K for acetaldehyde-dosed Pt(111) is replaced by reaction-limited H_2 peaks between 375 and 550 K for Zn/Pt(111). As shown in Figure 7, we postulate that the Zn adatoms play a direct role in formation and stabilization of the η_2(C,O) aldehyde intermediate by providing the bonding site for the O with the carbonyl carbon interacting with an adjacent Pt. This scenario is consistent with the high affinity of Zn for oxygen

dx.doi.org/10.1021/cs400355e | ACS Catal. 2013, 3, 1739−1750

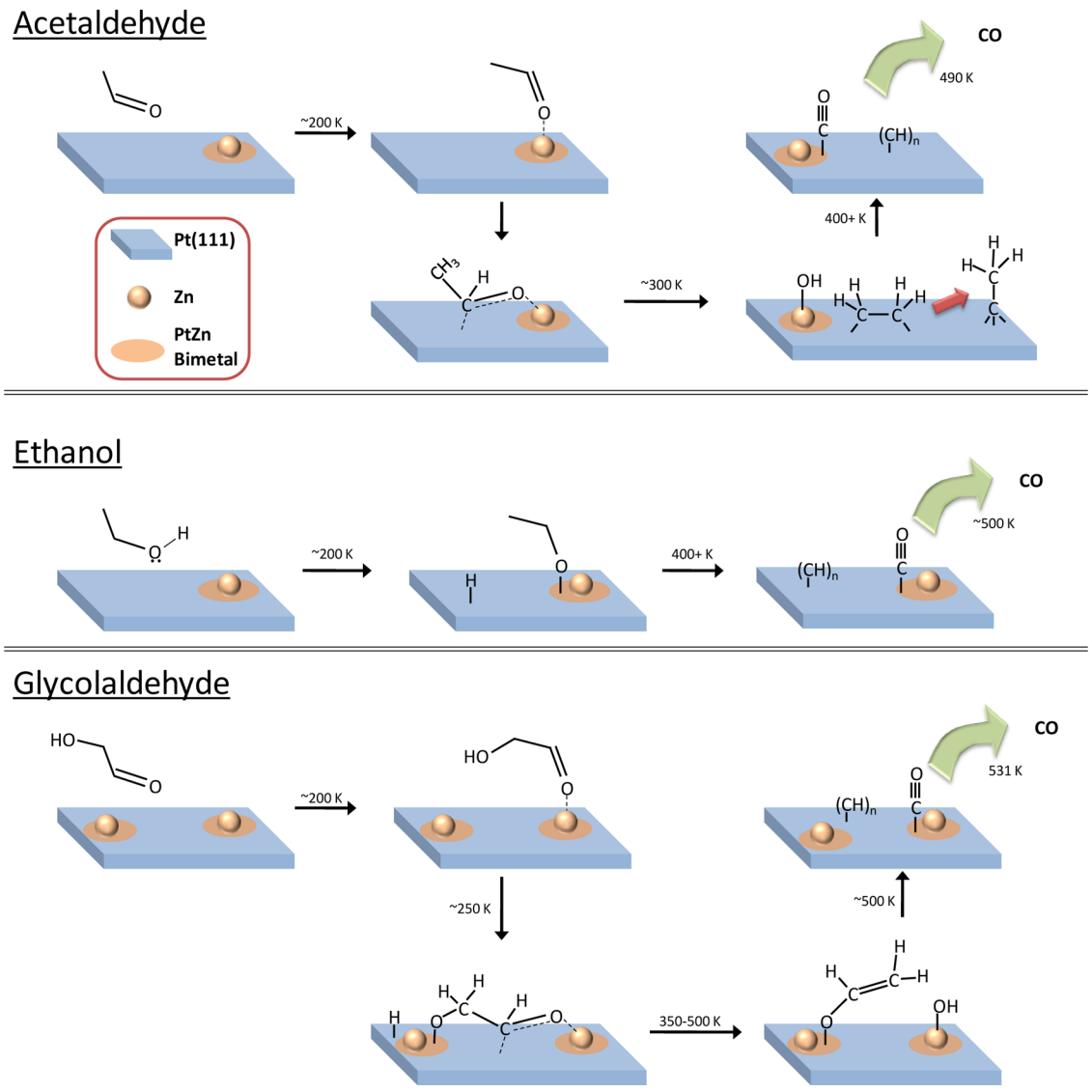

Figure 7. Proposed pathways and intermediates for the adsorption and reaction of acetaldehyde, ethanol, and glycolaldehyde on Zn/Pt(111) adatom surfaces.

and the observation of Zn oxidation (as determined by XPS) by Zn-bound methoxides on methanol-dosed Zn/Pt(111).[18]

The HREELS data show the formation of adsorbed hydroxyls upon heating the η_2(C,O) aldehyde intermediate to between 300 and 400 K providing definitive evidence for C−O bond scission. This is an important result since it could provide a pathway for selective deoxygenation of biomass-derived oxygenates which contain aldehyde functionalities, such as glucose or furfural. In the case of acetaldehyde, this deoxygenation pathway produces ethylene and ethylidyne intermediates (Figure 7) which during TPD ultimately decompose to carbon and hydrogen. Recognize, however, that under steady-state hydrodeoxygenation conditions these intermediates are likely to be hydrogenated to produce stable hydrocarbon products with the hydroxyls reacting to form water.

It is interesting that during acetaldehyde TPD on the Zn/Pt(111) surfaces where C−O scission occurred, a sharp Zn desorption peak was observed at 660 K. During TPD in the absence of other adsorbed species, the Zn adatoms on Zn/Pt(111) become incorporated into the surface upon heating to ~600 K and then desorb at higher temperatures. We speculate that the OH groups that are formed on Zn adatoms during acetaldehyde decomposition prevent the Zn from becoming incorporated into the surface and thus facilitate their desorption at a lower temperature.

The TPD and HREELS data for glycolaldehyde on Zn/Pt(111) indicate mechanistic similarities to that observed for acetaldehyde, including increased barriers for C−H bond activation, an η_2(C,O) aldehyde intermediate in which the O interacts with a Zn adatom, and C−O bond scission between 300 and 400 K. It is important to recognize for glycolaldehyde that it is feasible for C−O scission to occur at either the alcohol or the aldehyde functionalities. Data for the reaction of methanol[18] and ethanol on Zn/Pt(111) surfaces, however, argue for the latter. For all three molecules, methanol, ethanol, and glycolaldehyde, HREELS shows low-temperature O−H scission and a shift in the ν(C−O) peak, which is indicative of the formation of an alkoxide; although, for methanol and ethanol (Figure 6) C−O scission at the alkoxide moiety is not observed, thus it would also not be expected for glycolaldehyde. Furthermore, in our previous study of the reaction of methanol

dx.doi.org/10.1021/cs400355e | ACS Catal. 2013, 3, 1739−1750

on Zn/Pt(111), it was demonstrated that O−H scission was facilitated by the Zn adatoms.[18] Combined these results indicate the formation of the α-oxo-η_2 glycolaldehyde intermediate shown in Figure 7. Analogous to acetaldehyde, the carbonyl group in this species undergoes C−O scission upon heating to 350 K. For glycolaldehyde this results in the formation of a vinyl alkoxide intermediate. Evidence for this includes the ν(C═C) stretch at 1568 cm^{-1} as well as the strengthening of a ρ(CH) rocking mode at 1216 cm^{-1}, features common for surface bound vinyl groups.[47−49] Though vinyl groups are normally quite reactive on Pt surfaces, the geometric constraints imposed by the alkoxide surface linkage likely prevent the π electrons of the vinyl from interacting with the surface.

As shown schematically in Figure 8a, on group 10 metals (Ni, Pd, Pt) aldehydes typically undergo C−H scission to form acyl

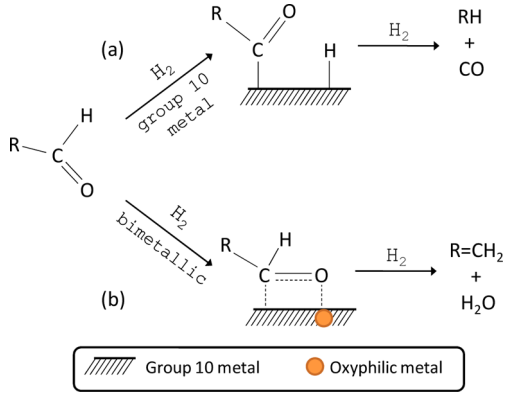

Figure 8. Reaction pathways for aldehydes and hydrogen on (a) group 10 metals and (b) bimetallics composed of a group 10 metal and a second more oxyphilic metal, for example, FeNi or PtZn.

intermediates followed by decarbonylation to form a hydrocarbon and CO.[16,32,42] The TPD and HREELS data obtained in this study demonstrate this pathway for both acetaldehyde and glycolaldehyde on Pt(111). In the context of upgrading oxygenates produced from biomass, such as glucose and furfural, to useful fuels and chemicals, this pathway generally needs to be avoided since it results in the loss of a carbon atom. Selective deoxygenation pathways, especially those involving carbonyl groups, are much more desirable since they produce more stable molecules with higher octane numbers. As noted in the introduction, alloying a highly active group 10 metal with a second, less-reactive metal has been proposed as one approach to alter the decarbonylation/deoxygenation selectivity to favor the deoxygenation pathway.[31,32] The recent study by Sitthisa et al. of the reaction of furfural and H_2 over Ni and NiFe bimetallic catalysts provides an excellent demonstration of this.[32] They observed that a Ni/SiO_2 catalyst was highly selective for decarbonylation to produce furan (C_4H_4O) and CO. In contrast, over a NiFe/SiO_2 catalyst, decarbonylation was significantly suppressed and the primary product was 2-methylfuran, which is produced via hydrogenolysis of the carbonyl group. On the basis of DFT calculations, they proposed that the reduction in decarbonylation was due to stabilization of an η_2(C,O) furfural intermediate via interaction of the carbonyl oxygen with an oxyphilic Fe atom and that this bonding configuration results in a weakening of the C−O bond thereby facilitating its dissociation.

The Zn/Pt(111) system is similar to the NiFe catalysts studied by Sitthisa et al.[32] in that it consists of a group 10 metal, Pt, modified by a less reactive oxyphilic metal, Zn. Our results for the reaction of both acetaldehyde and glycolaldehyde on Zn/Pt(111) are also consistent with those in the Sitthisa et al.[32] study and, furthermore, provide direct experimental confirmation of their proposed mechanism. In particular, as shown in Figure 8b, the addition of the second oxyphilic metal, Zn, was found to both provide a bonding site for the carbonyl oxygen, and increase the barrier for C−H bond scission, which is required for the formation of the acyl intermediate in the decarbonylation pathway. Combined, these factors lead to the formation of stable η_2(C,O) intermediates which are susceptible to C−O bond cleavage.

CONCLUSIONS

The TPD and HREELS results for the reaction of acetaldehyde and glycolaldehyde on Zn-modified Pt(111) surfaces obtained in this study lead to the following general conclusions: (1) alloying Pt with Zn decreases the activity for C−H and C−C bond cleavage, thereby stabilizing adsorbed oxygenate intermediates to higher temperatures; (2) the increased barriers for C−H bond scission on PtZn/Pt(111) and Zn/Pt(111) surfaces hinder the formation of acyl intermediates from adsorbed aldehydes, which effectively decreases the selectivity for decarbonylation; (3) interaction of the carbonyl oxygen with Zn atoms stabilizes aldehyde bonding in an η_2(C,O) configuration, facilitating selective C−O bond cleavage at higher temperatures via the weakening of the C═O bond relative to that in the parent aldehyde. In addition to elucidating how Zn alters the reactivity of Pt toward aldehydes, the mechanistic insights obtained in this study are useful for the design of catalysts that are active for the selective deoxygenation of the aldehyde functionalities in biomass-derived oxygenates, such as glucose and furfural.

AUTHOR INFORMATION

Corresponding Author

*E-mail: Vohs@seas.upenn.edu.

Notes

The authors declare no competing financial interest.

ACKNOWLEDGMENTS

This work was supported as part of the Catalysis Center for Energy Innovation, an Energy Frontier Research Center funded by the U.S. Department of Energy, Office of Science, Office of Basic Energy Sciences under award no. DE-SC0001004.

ABBREVIATIONS

DFT, density functional theory; HDO, hydrodeoxygenation; HREELS, high-resolution electron energy loss spectroscopy; QCM, quartz crystal microbalance; TPD, temperature programmed desorption; UHV, ultrahigh vacuum; XPS, X-ray photoelectron spectroscopy

REFERENCES

(1) Bulushev, D. A.; Ross, J. R. H. *Catal. Today* **2011**, *171*, 1−13.
(2) Huber, G. W.; Iborra, S.; Corma, A. *Chem. Rev.* **2006**, *106*, 4044−4098.
(3) Stocker, M. *Angew. Chem., Int. Ed.* **2008**, *47*, 9200−9211.
(4) Alonso, D. M.; Wettstein, S. G.; Dumesic, J. A. *Chem. Soc. Rev.* **2012**, *41*, 8075−8098.

(5) Chen, J. G.; Menning, C. A.; Zellner, M. B. *Surf. Sci. Rep.* **2008**, *63*, 201−254.
(6) Chia, M.; Pagan-Torres, Y. J.; Hibbitts, D.; Tan, Q. H.; Pham, H. N.; Datye, A. K.; Neurock, M.; Davis, R. J.; Dumesic, J. A. *J. Am. Chem. Soc.* **2011**, *133*, 12675−12689.
(7) Skoplyak, O.; Barteau, M. A.; Chen, J. G. G. *J. Phys. Chem. B* **2006**, *110*, 1686−1694.
(8) Skoplyak, O.; Barteau, M. A.; Chen, J. G. G. *Surf. Sci.* **2008**, *602*, 3578−3587.
(9) Skoplyak, O.; Barteau, M. A.; Chen, J. G. G. *Catal. Today* **2009**, *147*, 150−157.
(10) Skoplyak, O.; Menning, C. A.; Barteau, M. A.; Chen, J. G. G. *J. Chem. Phys.* **2007**, *127*, 114707−114718.
(11) McManus, J. R.; Vohs, J. M. *Appl. Surf. Sci.* **2013**, *271*, 45−51.
(12) Do, P. T. M.; Foster, A. J.; Chen, J. G.; Lobo, R. F. *Green Chem.* **2012**, *14*, 1388−1397.
(13) Yang, Y.; Du, Z.; Huang, Y.; Lu, F.; Wang, F.; Gao, J.; Xu, J. *Green Chem.* **2013**, *15*, 1932−1940.
(14) Jiang, T.; Zhou, Y. X.; Liang, S. G.; Liu, H. Z.; Han, B. X. *Green Chem.* **2009**, *11*, 1000−1006.
(15) Liu, H. Z.; Liang, S. G.; Jiang, T.; Han, B. X.; Zhou, Y. X. *Clean: Soil, Air, Water* **2012**, *40*, 318−324.
(16) Zhou, J. X.; Guo, L. Y.; Guo, X. W.; Mao, J. B.; Zhang, S. G. *Green Chem.* **2010**, *12*, 1835−1843.
(17) Xia, S. X.; Yuan, Z. L.; Wang, L. N.; Chen, P.; Hou, Z. Y. *Appl. Catal., A* **2011**, *403*, 173−182.
(18) Martono, E.; Vohs, J. M. *J. Phys. Chem. C* **2013**, *117*, 6692−6701.
(19) Conant, T.; Karim, A. M.; Lebarbier, V.; Wang, Y.; Girgsdies, F.; Schlogl, R.; Datye, A. *J. Catal.* **2008**, *257*, 64−70.
(20) Iwasa, N.; Masuda, S.; Ogawa, N.; Takezawa, N. *Appl. Catal., A* **1995**, *125*, 145−157.
(21) Jeroro, E.; Hyman, M. P.; Vohs, J. M. *Phys. Chem. Chem. Phys.* **2009**, *11*, 10457−10465.
(22) Jeroro, E.; Vohs, J. M. *J. Am. Chem. Soc.* **2008**, *130*, 10199−10207.
(23) Jeroro, E.; Vohs, J. M. *Catal. Lett.* **2009**, *130*, 271−277.
(24) Jeroro, E.; Vohs, J. M. *J. Phys. Chem. C* **2009**, *113*, 1486−1494.
(25) Rameshan, C.; Weilach, C.; Stadlmayr, W.; Penner, S.; Lorenz, H.; Havecker, M.; Blume, R.; Rocha, T.; Teschner, D.; Knop-Gericke, A.; Schlogl, R.; Zemlyanov, D.; Memmel, N.; Rupprechter, G.; Klotzer, B. *J. Catal.* **2010**, *276*, 101−113.
(26) Neyman, K. M.; Lim, K. H.; Chen, Z. X.; Moskaleva, L. V.; Bayer, A.; Reindl, A.; Borgmann, D.; Denecke, R.; Steinruck, H. P.; Rosch, N. *Phys. Chem. Chem. Phys.* **2007**, *9*, 3470−3482.
(27) Rodriguez, J. A.; Kuhn, M. *J. Chem. Phys.* **1995**, *102*, 4279−4289.
(28) Stadlmayr, W.; Rameshan, C.; Weilach, C.; Lorenz, H.; Havecker, M.; Blume, R.; Rocha, T.; Teschner, D.; Knop-Gericke, A.; Zemlyanov, D.; Penner, S.; Schlogl, R.; Rupprechter, G.; Klotzer, B.; Memmel, N. *J. Phys. Chem. C* **2010**, *114*, 10850−10856.
(29) Tsai, A. P.; Kameoka, S.; Ishii, Y. *J. Phys. Soc. Jpn.* **2004**, *73*, 3270−3273.
(30) Nishiyama, S.; Hara, T.; Tsuruya, S.; Masai, M. *J. Phys. Chem. B* **1999**, *103*, 4431−4439.
(31) Hirschl, R.; Delbecq, F.; Sautet, P.; Hafner, J. *J. Catal.* **2003**, *217*, 354−366.
(32) Sitthisa, S.; An, W.; Resasco, D. E. *J. Catal.* **2011**, *284*, 90−101.
(33) Alonso, D. M.; Bond, J. Q.; Dumesic, J. A. *Green Chem.* **2010**, *12*, 1493−1513.
(34) Liu, D. X.; Zemlyanov, D.; Wu, T. P.; Lobo-Lapidus, R. J.; Dumesic, J. A.; Miller, J. T.; Marshall, C. L. *J. Catal.* **2013**, *299*, 336−345.
(35) Ammari, F.; Lamotte, J.; Touroude, R. *J. Catal.* **2004**, *221*, 32−42.
(36) McManus, J. R.; Salciccioli, M.; Yu, W. T.; Vlachos, D. G.; Chen, J. G. G.; Vohs, J. M. *J. Phys. Chem. C* **2012**, *116*, 18891−18898.
(37) McManus, J. R.; Yu, W. T.; Salciccioli, M.; Vlachos, D. G.; Chen, J. G. G.; Vohs, J. M. *Surf. Sci.* **2012**, *606*, L91−L94.
(38) Ho, C.-S.; Martono, E.; Banerjee, S.; Roszell, J.; Vohs, J. M.; Koel, B. E. *J. Phys. Chem. A* **2013**, DOI: 10.1021/jp4006668.
(39) Zhao, H. B.; Kim, J.; Koel, B. E. *Surf. Sci.* **2003**, *538*, 147−159.
(40) Evans, J. C.; Bernstein, H. J. *Can. J. Chem.* **1956**, *34*, 1083−1092.
(41) Delbecq, F.; Vigne, F. *J. Phys. Chem. B* **2005**, *109*, 10797−10806.
(42) Davis, J. L.; Barteau, M. A. *J. Am. Chem. Soc.* **1989**, *111*, 1782−1792.
(43) Steininger, H.; Ibach, H.; Lehwald, S. *Surf. Sci.* **1982**, *117*, 685−698.
(44) Yagasaki, E.; Backman, A. L.; Masel, R. I. *J. Phys. Chem.* **1990**, *94*, 1066−1072.
(45) Anson, C. E.; Sheppard, N.; Powell, D. B.; Norton, J. R.; Fischer, W.; Keiter, R. L.; Johnson, B. F. G.; Lewis, J.; Bhattacharrya, A. K.; Knox, S. A. R.; Turner, M. L. *J. Am. Chem. Soc.* **1994**, *116*, 3058−3062.
(46) Liu, Z. M.; Zhou, X. L.; Buchanan, D. A.; Kiss, J.; White, J. M. *J. Am. Chem. Soc.* **1992**, *114*, 2031−2039.
(47) Pursell, D. P.; Bocquet, M. L.; Vohs, J. M.; Dai, H. L. *Surf. Sci.* **2003**, *522*, 90−104.
(48) Zaera, F.; Bernstein, N. *J. Am. Chem. Soc.* **1994**, *116*, 4881−4887.
(49) Zaera, F.; Hall, R. B. *Surf. Sci.* **1987**, *180*, 1−18.
(50) Hatzikos, G. H.; Masel, R. I. *Surf. Sci.* **1987**, *185*, 479−494.
(51) Bent, B. E.; Mate, C. M.; Crowell, J. E.; Koel, B. E.; Somorjai, G. A. *J. Phys. Chem.* **1987**, *91*, 1493−1502.
(52) Gates, J. A.; Kesmodel, L. L. *Surf. Sci.* **1983**, *124*, 68−86.
(53) Malik, I. J.; Brubaker, M. E.; Mohsin, S. B.; Trenary, M. *J. Chem. Phys.* **1987**, *87*, 5554−5561.
(54) Slavin, A. J.; Bent, B. E.; Kao, C. T.; Somorjai, G. A. *Surf. Sci.* **1988**, *202*, 388−404.
(55) Ibach, H.; Lehwald, S. *J. Vac. Sci. Technol.* **1978**, *15*, 407−415.
(56) Davis, J. L.; Barteau, M. A. *Surf. Sci.* **1990**, *235*, 235−248.
(57) Sbrana, G.; Schettin., V. *J. Mol. Spectrosc.* **1970**, *33*, 100−108.
(58) Jetzki, M.; Luckhaus, D.; Signorell, R. *Can. J. Chem.* **2004**, *82*, 915−924.
(59) Jeroro, E.; Lebarbler, V.; Datye, A.; Wang, Y.; Vohs, J. M. *Surf. Sci.* **2007**, *601*, 5546−5554.